THE JOURNAL OF BIOLOGICAL CHEMISTRY
Vol. 274, No. 52, Issue of December 24, pp. 37370–37378, 1999
Printed in U.S.A.

The Zinc Finger Cluster Domain of RanBP2 Is a Specific Docking Site for the Nuclear Export Factor, Exportin-1*

(Received for publication, May 7, 1999, and in revised form, September 18, 1999)

Brij B. Singh, Hemal H. Patel, Ronald Roepman‡, Diana Schick, and Paulo A. Ferreira§

From the Department of Pharmacology and Toxicology, Medical College of Wisconsin, Milwaukee, Wisconsin 53226 and the ‡Department of Human Genetics, University Hospital Nijmegen, 6500 HB Nijmegen, The Netherlands

The Ran-binding protein 2 (RanBP2) is a large scaffold cyclophilin-related protein expressed in photoreceptor cells. Red/green opsin, Ran-GTPase, and the 19 S regulatory complex of the proteasome associate with specific RanBP2 structural modules. Some of these play a role in chaperoning the functional expression of opsin. RanBP2 localization at cytoplasmic fibrils emanating from the nuclear pore complex and interaction with the Ran-GTPase support also its role in nucleocytoplasmic transport processes. The degenerate nucleoporin repeat motifs FXFG, GLFG, and XXFG have been proposed to mediate the movement of nucleocytoplasmic transport factors. In particular, RanBP2 has been implicated in nuclear import processes. Here, we show the zinc fingers of RanBP2 associate with high specificity to the nuclear export factor, exportin-1 (CRM1). The bovine RanBP2 transcript contained only five of the eight zinc fingers reported in the human counterpart and are sufficient for exportin-1 association with RanBP2. In contrast to Ran interaction with RanBP2-exportin-1 complex, exportin-1 binding to the zinc finger cluster domain of RanBP2 is insensitive to leptomycin B and nucleotide-bound state of Ran-GTPase. Our results indicate that the zinc finger-rich domain of RanBP2 constitutes a docking site for exportin-1 during nuclear export. Thus, RanBP2 emerges as a key component of the nuclear export pathway.

Protein machines are composed of assemblies of many distinct protein molecules (1). Many are ubiquitous throughout cells, and emerging evidence shows that networks of intertwining protein machines underline many cellular processes. Protein complexes allow channeling of substrates and, consequently, compartmentalization of biological activity in an extremely coordinated and efficient manner. Furthermore, protein-protein interactions within protein machines allow biological processes to be tightly regulated. Whereas many of these protein-protein interactions occur in a stable fashion, others may be transient in nature. This allows the fluid recruitment of substrates into higher order complexes and modulation of biological responses.

The retinal Ran-binding protein 2 (RanBP2)[1] is a scaffold protein composed of multiple, distinct, and well defined structural modules mediating, singly or in combination, the recruitment of protein machines (*e.g.* regulatory subunits of the 26 S proteasome) (2) and molecular switches (*e.g.* Ran-GTPase) (3–5) possibly involved in protein biogenesis (*e.g.* red/green opsins) in cone photoreceptors (3, 6). The ubiquitin (SUMO-1)-like modified Ran-GTPase-activating protein appears also to associate with RanBP2 (7–10). We have shown that the combination of Ran-binding domain 4 and cyclophilin domains are required to enhance *in vivo* the production of functional opsin receptor (3) and generate an opsin isoform with low propensity to self-aggregate. In addition, the 19 S regulatory subunits of the proteasome associated specifically and selectively in retinal tissue with the cyclophilin-like domain (CLD) of RanBP2 (2, 4). To this end, we have proposed that the association of RanBP2 with the proteasome may lead to the processing of RanBP2 and production of at least another smaller RanBP2 isoform in retinal cells (2). Altogether these results suggest that at least some subunits of the 19 S cap of the proteasome may play a selective surveillance role during the processing of opsins and RanBP2.

RanBP2 appears to belong to a large family of proteins, nucleoporins, due to its localization at the vicinity of the nuclear pore complex (NPC) (5, 11, 12). Other "atypical" proteins have been also localized at the NPC, such as Sec13p (and the related, Seh1p) (13), a protein involved in endoplasmic reticulum to Golgi transport (14). Nucleoporins are characterized, albeit not exclusively, for the presence of the degenerate peptide-repeat motifs, FXFG, GLFG, and/or XXFG (11). RanBP2 contains FXFG signature repeats (5, 12, 15) and associates with Ran in a GTP-dependent fashion via interaction with its Ran-binding domains (3–5, 16) homologous to the small Ran-binding protein, RanBP1 (17). RanBP1 stabilizes Ran-GTP (18, 19) and, together with the cytosolic Ran-GTPase-activating protein, increases the hydrolysis of Ran-GTP (19, 20).

Ran-GTPase is shuttled between the nucleus and cytoplasm (21–23). Ran is critical in coordinating the nuclear import (24, 25) and export (26–28) of substrates. Their import and export are, in part, coded by signature sequences in the substrates and

* This work was supported by National Institutes of Health Grant EY11993, the Karl Kirchgessner Foundation, and Fight for Sight, Inc. (to P. A. F.). The costs of publication of this article were defrayed in part by the payment of page charges. This article must therefore be hereby marked "*advertisement*" in accordance with 18 U.S.C. Section 1734 solely to indicate this fact.

The nucleotide sequence(s) reported in this paper has been submitted to the GenBank™/EBI Data Bank with accession number(s) AJ133723.

§ To whom correspondence should be addressed: Dept. of Pharmacology and Toxicology, Medical College of Wisconsin, 8701 Watertown Plank Rd., Milwaukee, WI 53226. Tel.: 414-456-8877; Fax: 414-456-6545; E-mail: ferreira@post.its.mcw.edu.

[1] The abbreviations used are: RanBP2, Ran-binding protein 2; ZnF, zinc fingers; ZnF-BP, zinc finger-binding protein; kb, kilobase pair; RT-PCR, reverse transcriptase-polymerase chain reaction; CHAPS, 3-[(3-cholamidopropyl)dimethylammonio]-1-propanesulfonic acid; GST, glutathione *S*-transferase; MALDI, matrix-assisted laser desorption ionization; TOF, time of flight; MS, mass spectrometer; DTT, dithiothreitol; PAGE, polyacrylamide gel electrophoresis; CLD, cyclophilin-like domain; NES, nuclear export signals; NPC, nuclear pore complex; TPEN, *N*,*N*,*N*′,*N*′-tetrakis(2-pyridylmethyl)ethylenediamine; LMB, leptomycin B; HPLC, high pressure liquid chromatography; CY, cyclophilin; GTPγS, guanosine 5′-3-*O*-(thio)triphosphate; ATPγS, adenosine 5′-*O*-(thiotriphosphate); AMP-PNP, adenosine 5′-(β,γ-imino)triphosphate; CCR, central conserved region.

designated as, respectively, nuclear localization signals (29) and leucine-rich nuclear export signals (NES) (30–33). The former associate with nuclear import receptors such as importins (importin-α) and karyopherins (23, 34), and the latter associate with the nuclear export receptors, exportins (35). The cellular apoptosis susceptibility protein (36) is also an exportin-related protein; however, it appears particularly to be required in export of importin-α (37). Another class of escort proteins, transportins (38, 39), are nuclear import receptors of substrates containing the noncanonical nuclear export and import signal, M9, present for example in human ribonucleoprotein A1 (40, 41).

The vectorial nature of the nuclear transport is based on a proposed nuclear-to-cytoplasm Ran-GTP to Ran-GDP asymmetric distribution of Ran-GTPase. The nucleotide-bound state of Ran, in concert with transport proteins, mediates the vectorial nucleocytoplasmic delivery of substrates (27, 28, 42). In particular, RanBP2 has been proposed to participate in the nuclear import of proteins based on the nuclear import inhibition of a test substrate upon injection of an anti-RanBP2 antibody into cytoplasm of HeLa cells (5). The nucleocytoplasmic movement of substrates has been proposed to occur via a stochastic process through reiterated steps of docking-undocking reactions between degenerate F*X*FG, and GLFG, repeats of nucleoporins and subunits of nuclear transport factors (43, 44).

To understand better the role of RanBP2 in nucleocytoplasmic transport and retinal function, we have taken a novel systematic approach in isolating and identifying components that interact specifically with selective and well defined domains of RanBP2 (2–4, 6). Here, we report that the zinc finger cluster domain of bovine RanBP2 associates with high specificity to the conserved chromosome region maintenance protein 1, CRM1 (45). This protein was found to shuttle between the nucleus and cytoplasm mediating the export of substrates containing nuclear export signals (NES) (46–50) and thereby was renamed exportin-1 (50). Thus, the zinc finger cluster domain of RanBP2 likely constitutes a cytoplasmic docking domain for the delivery of nuclear cargo transported by exportin-1 to the cytoplasmic machinery. We discuss the implications of these findings on RanBP2 function in nucleocytoplasmic export and protein kinesis and biogenesis.

MATERIALS AND METHODS

Molecular Cloning of Zinc Finger Cluster Motifs—The ~1.5- and 1.9-kb bovine and human zinc finger domain cDNAs, respectively, were isolated at least four times by RT-PCR of bovine and human tissues and mRNA of cells as indicated. Poly(A^+) RNA was extracted directly from bovine retinas using the Poly(A) Tract System 1000 (Promega) as directed by the manufacturer. First strand cDNA synthesis was carried out with 1 μg of mRNA using the antisense-specific primer against the 5′-end of bovine Ran-binding domain-2 (RBD2), 5′-GTCCTCAGTCTTATAGGCATCATC. This reverse primer and the forward primer, 5′-GAATTTCAGGTTGCAAAGAAAGAAG, against the 3′-sequence of Ran-binding domain-1 (RBD1) were derived from cDNA clones comprising RBD2 and RBD1 domains of bovine RanBP2 that were isolated from the screening of a randomly primed bovine retinal cDNA library using two-hybrid and standard library screening procedures.[2] These primers were also 100% identical to the RanBP2 sequence isolated from HeLa and lymphocyte cells. RT-PCR was performed using SuperScript reverse transcriptase II (Life Technologies, Inc.) as recommended by the manufacturer. PCR reactions contained 20 mM Tris-HCl, pH 8.5, 50 mM KCl, 1.5 mM $MgCl_2$, 0.2 mM concentration of dNTP, 20 pmol of each amplification primer, first strand cDNA, and 2.5 units of *Taq* DNA polymerase. Thirty five cycles of PCR were performed at the following conditions: 94 °C denaturation for 30 s, 55 °C annealing for 45 s, and 68 °C extension for 3 min. PCR products were separated on a 1% agarose gel. The ~1.5-kb bovine retinal cDNA product was eluted and subcloned into a TA cloning vector (Invitrogen). The *Eco*RI fragment having ~1.5-kb gene product was double-strand sequenced and subcloned in-frame into the pGEX-KG (77) vector digested with *Eco*RI. At least 10 clones were analyzed for the right orientation of the insert. Similarly, the ~1.9-kb cDNA products from mRNA of human retinas and HeLa cells were isolated by the same exact methods, conditions, and primers. At least two bovine cDNA clones were double-strand sequenced using standard sequencing methods to overcome nucleotide mis-incorporation occurred by PCR.

Radiation Hybrid Mapping of the Zinc Finger Cluster Domain of RanBP2—Radiation hybrid mapping was performed with the Stanford G3 Radiation Hybrid Panel (Research Genetics). PCR reactions were performed in a volume of 10 μl using 25 ng of DNA of each hamster/human hybrid cell line, 4 pmol of primer 2740 (gtgcttagtaagaaatgaagc, specific for zinc fingers 5–7) and primer 2741 (cttagtgaacattccctcaaa, reverse primer, specific for zinc fingers 4–6), 10 mM Tris-HCl, pH 8.3, 50 mM KCl, 1.5 mM $MgCl_2$, 5 mM DTT, 0.2 mM of each dNTP, and 0.4 units of *Taq* DNA polymerase (Life Technologies, Inc.). Amplification was performed for 35 cycles at 95 °C for 30 s, 56 °C for 45 s, and 72 °C for 1 min in an ABI 9600 thermal cycler (Perkin-Elmer). The localization of the cDNA fragments in the Stanford G3 Radiation Hybrid Map was determined at the Stanford Human Genome Center. The highest LOD scores were obtained for the markers SHGC-1639 (LOD score 7.82, DIST. 24 cRs) and SHGC-37095 (LOD score 5.71, DIST. 36 cRs) on chromosome 2 (51, 52), which correlates with chromosome 2 map positions 251 and 255, respectively. RanBP2 was previously linked to SHGC-36406, in reference interval D2S293-D2S121 (122.4–127.9 centimorgans), which correlates to chromosome 2 map position 252–265, thus confirming the mapping results of the zinc finger domain.

Expression of GST-Zinc Finger Motifs of Bovine RanBP2—Expression of GST fusion and GST-cleaved proteins was carried out as described previously (4, 77) with the following exceptions. *Escherichia coli*-expressing cultures were supplemented with 60 μM $ZnSO_4$ at the time of induction. The cell pellet was resuspended in PBST buffer (4) without EDTA and supplemented with 100 μM $ZnSO_4$ and 2 mM Pefabloc (Roche Molecular Biochemicals). Cells were lysed by passing the cell suspension through a French press at 1200 pounds/square inch. Cell debris was removed by centrifugation at 11,000 × *g* for 15 min. The supernatant was loaded on a glutathione *S*-agarose affinity column (Amersham Pharmacia Biotech), and protein purification was carried out on an AKTA explorer FPLC system (Amersham Pharmacia Biotech). All buffers were supplemented with 60 μM $ZnSO_4$.

Analytical GST-ZnF Binding Assays—Incubation reactions of GST-fused constructs (2.2 μM) with CHAPS-solubilized bovine retinal extracts (~2.5 mg of total protein) were carried out exactly as described previously (2–4, 6). The other tissue extracts (liver, brain, and spleen) were prepared similarly to that of retina, and GST pull-down assays were performed similarly using ~2.5 mg of total protein. Chicken retinal extracts reactions contained about 1.2 mg of total protein extract and 2.2 μM GST-fused construct. When applicable, nonhydrolyzable nucleotides (Sigma) were added at a concentration of 400 μM. Unfused construct (competitor) was used at 5-fold molar excess, except with RBD4, where a 10-fold molar of unfused protein was used. For exportin-1 elution assays, EDTA, DTT, and/or TPEN were added to the washed pellets of incubation reactions at a concentration of 50, 10, and 5 mM, respectively, for 10 min at 4 °C. Zn^{2+}-ZnF reconstitution assays were carried out by incubating GST-ZnF with retinal extracts, washing of the coprecipitates, elution of exportin-1 with 1 mM TPEN for 10 min at 4 °C followed by the addition of Zn^{2+} ($ZnSO_4$) at different concentrations for 30 min at 24 °C and SDS-PAGE analysis of the pellets and supernatants of the incubation reactions. Leptomycin B was dissolved in Me_2SO and used at 250 nM concentration. All coprecipitates were analyzed on 7.5% SDS-PAGE after boiling in SDS sample buffer with exception of those reactions shown in Fig. 6 that were analyzed in a 12% SDS-PAGE. When applicable, the proteasome inhibitors, lactacystine and MG132 (Biomol), were used at 20 nM and 20 μM, respectively.

Purification of Retinal 110-kDa ZnF-binding Protein—For purification of retinal 110-kDa ZnF-binding protein, analytical reactions were scaled up to ~500-fold between 18 15-ml conical tubes. The washings of coprecipitates were scaled up accordingly, and the divalent cations, Ca^{2+} and Mg^{2+}, were omitted in the regular washing buffer (2–4, 6). After subsequent washing the samples were supplemented with 50 mM EDTA, 10 mM DTT, and 1 mM TPEN and were incubated for 10 min at 4 °C. The reactions were subjected to rapid centrifugation (10,000 rpm, 1 min) and the supernatant was collected. To avoid contamination of GST beads along with GST-fused protein, CytoSignal-spin filters (CytoSignal, CA) were used to filtrate the supernatant through a mesh that retains the contaminating glutathione *S*-agarose beads. The remaining beads were again incubated with EDTA, DTT, and TPEN, and the

[2] P. A. Ferreira *et al.*, manuscript in preparation.

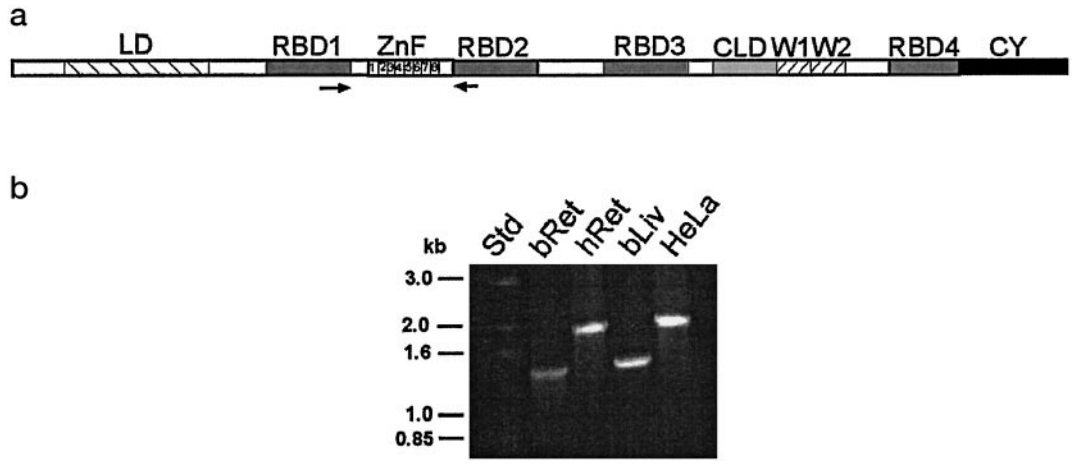

FIG. 1. *a,* schematic diagram of RanBP2 primary structure. RBDn = 1–4 are four repeat Ran-binding domains homologous to the small RanBP1 protein (3, 5, 12, 15, 75). *CY* is homologous to Nina A and other cyclophilin proteins (3, 5, 12, 75); *LD* and *ZnF* are, respectively, leucine-rich and zinc finger-rich domains (5, 12, 15); *CLD*, cyclophilin-like domain which associates specifically with the 19 S regulatory subunit of the proteasome (2, 75); *W1* and *W2*, internal repeats (5, 75). Primers used in this study for RT-PCR and cDNA amplification of zinc finger-rich domain of RanBP2 are 100% conserved in bovine, mouse, and human and are noted as *arrows*. *b,* RT-PCR of zinc finger cluster domain of RanBP2. 200 and 350 ng of mRNA from bovine and human tissues, respectively, was reversed-transcribed and cDNA-amplified with primers against the flanking domains, RBD1 and RBD2. Approximately half of the PCR products was analyzed on a 1% agarose gel. The ZnF cDNA fragments amplified from human retina (*hRet*) and HeLa (*HeLa*) cells were about 1.9 kb in size, whereas those from the bovine retina (*bRet*) and liver (*bLiv*) were just 1.5 kb. *Std*, DNA molecular weight standards.

supernatant was collected similarly as described. Eluted protein was concentrated in Centricon-50 and boiled in SDS sample buffer for 3 min and loaded on 6% SDS-PAGE. This was stained with Fast Stain followed by electroelution of P110 bands and mock (blank) neighboring gel bands into Centricons. Eluted samples were concentrated and buffer exchanged twice in 100 mM ammonium bicarbonate and then lyophilized. 5% (v/v) of the total concentrated and purified protein was resolved in SDS-PAGE in parallel with coprecipitates of analytical retinal binding reactions and analyzed by silver stain as described (2, 4). Trypsin digestion of the remaining protein and mock sample (1:50 of trypsin:substrate) was carried out overnight in 50 mM Tris, pH 7.8, at 27 °C. A small aliquot of the trypsin digest mixture was first screened by peptide mass mapping in a matrix-assisted laser desorption ionization-time of flight mass spectrometer (MALDI-TOF, Perkin-Elmer Voyager DE-Pro) and compared against protein data bases. The remaining trypsin digest mixture and mock sample were resolved by HPLC on a C18 reverse-phase column. All collected fractions were analyzed by MALDI for identification of purified peptides. Two fractions, numbers 37 and 53, were subjected to Edman degradation.

Western Blot Analysis of GST-ZnF Retinal Coprecipitates—GST-ZnF retinal coprecipitates were resolved on SDS-PAGE and blotted onto a polyvinylidene difluoride membrane, and Western blot analysis was carried out exactly as described previously (2, 4). CRM1/exportin-1 (gift from Dr. G. Grosveld) and Ran (Santa Cruz Laboratories) antiserum were used at 1:200 and 1:5,000 dilutions, respectively. Blots were developed in the presence of a chemiluminescent substrate (Super Signal, Pierce) for 5 min.

RESULTS

The Bovine RanBP2 Transcript Encodes a Protein with Five Zinc Finger Motifs—To generate a GST-fused construct containing the Zinc finger cluster domain of bovine RanBP2, RT-PCR was carried out on bovine retinal mRNA with primers against the flanking and conserved domains of bovine Ran-binding domains 1 and 2 (*RBD1* and *RBD2*, Fig. 1, *a* and *b*). Analysis of the size of PCR products (Fig. 1*b*) and nucleic acid sequence comparison of the bovine ZnF domain with the HeLa counterpart sequence showed that it contained only five out of the eight ZnF motifs previously reported in human RANBP2. (Fig. 2). The 5th and 6th and either the 4th or 7th fingers were absent in bovine retinal RanBP2 (Fig. 2). Moreover, the bovine 4th zinc finger is missing the 2nd cysteine. To investigate whether the lack of these fingers was due to species- or tissue-specific differences in RanBP2, RT-PCR was also performed with the same primers on bovine liver, human, retinal, and HeLa cell mRNAs (Fig. 1*b*). These results confirmed that the bovine *ranBP2* gene encodes a protein with only five zinc fingers in contrast to eight and six present in its human and mouse orthologues, respectively (5, 12, 15) (Fig. 2).

Sequence analysis of the zinc finger cluster domain of human RANBP2 revealed that the unique 5th and 6th zinc finger motifs, and their immediate downstream flanking sequences, were 100% identical to each other at nucleic acid level (Fig. 2*a*). To rule out unequivocally that these two motifs arose from a very recent "illegitimate" recombination event and the human RT-PCR product amplified was derived from the same human *RANBP2* gene previously mapped (51, 52), we physically mapped these Zinc finger motifs onto the human genome. Radiation hybrid mapping confirmed that the human zinc finger motifs amplified colocalized only in chromosome 2 at the same locus previously reported for the human *RANBP2* gene (51, 52).

The Zinc Finger Cluster Domain of RanBP2 Associates Specifically with a 110-kDa Retinal Protein—We continued the structure-function analysis of RanBP2 by focusing this time on the zinc finger cluster domain (ZnF) of RanBP2 (Fig. 1*a*). We used the bovine five zinc finger motifs of RanBP2 to screen for specific ZnF-interacting proteins in bovine retinal extracts by the same methods previously reported (2, 4). Briefly, this method consists of pull-down assays of retinal extract reactions incubated in the presence of GST-fused protein and, parallel reactions, coincubated with GST-fused, 5–10-fold of cleaved (unfused) protein. Retinal protein(s) that *specifically* associate with the fused protein moiety are identified among those with binding activity in incubation reactions with GST-fused protein but not in those with the combination of GST-fused and -cleaved (unfused) proteins (2, 4).

Comparison of incubation reactions of GST-ZnF and, GST-ZnF and unfused (free) ZnF, with retinal extracts followed by analysis of the coprecipitates by silver stain of SDS-polyacrylamide gels showed that a retinal protein with an apparent molecular mass of 110 kDa (ZnF-BP) associated with high specificity to GST-ZnF (Fig. 3*a*). This binding was highly specific because only the association of the novel ZnF-BP with GST-ZnF was completely disrupted in presence of free (unfused) ZnF (Fig. 3*a*). To test further the binding specificity of ZnF-BP to GST-ZnF, we carried out coincubation reactions in the presence of other free RanBP2 domains such as RBD4. To

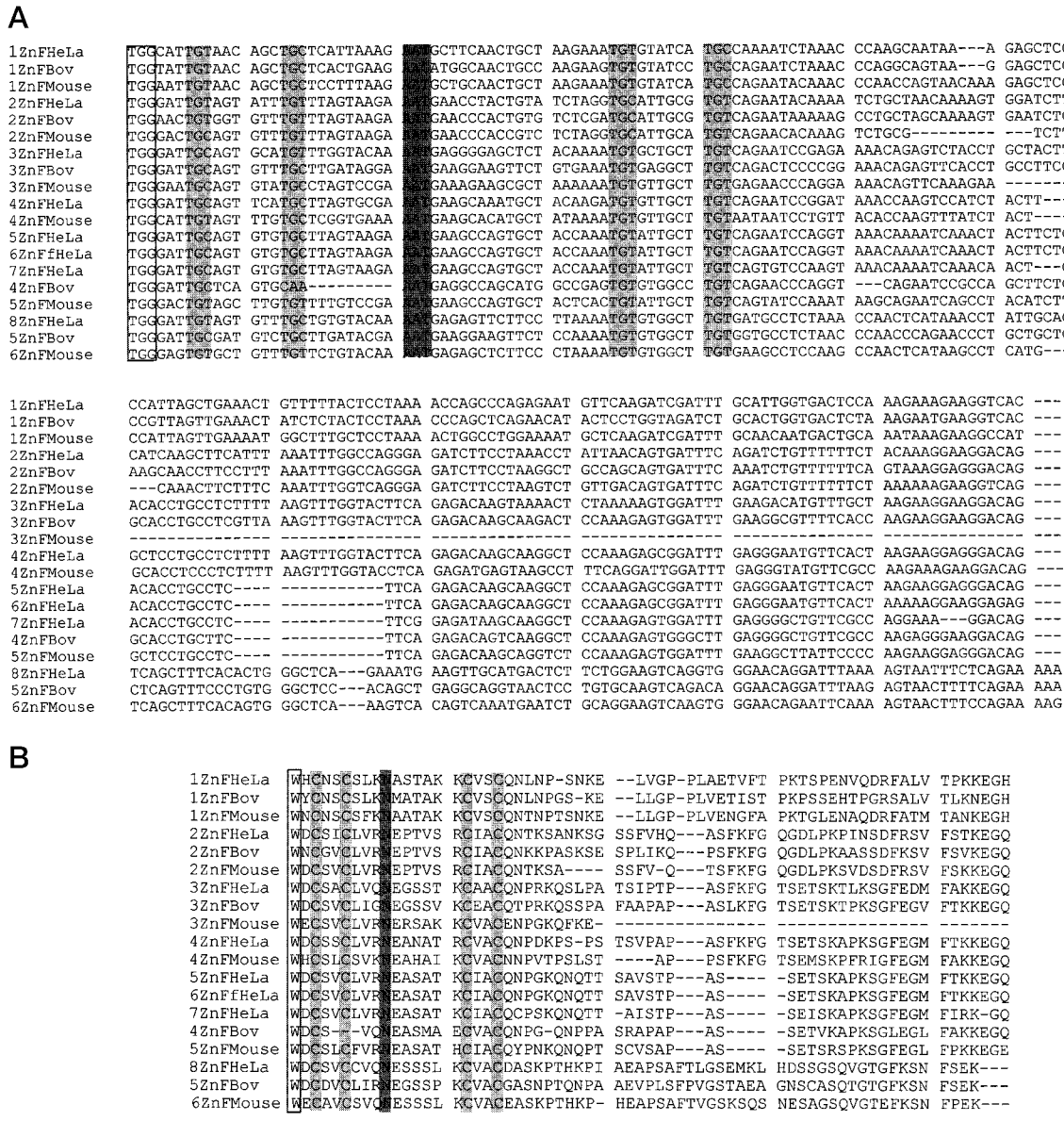

FIG. 2. **Sequence alignment of nucleic acid *(a)* and amino acid *(b)* sequences of zinc finger domains of bovine, human, and mouse RanBP2 isoforms.** Sequence analysis and multiple alignment of all Zn^{2+} fingers present in RanBP2 isoforms expressed in bovine retina (75), HeLa (12), and murine F9 cells (15) showed that the HeLa and murine RanBP2 isoforms contained, respectively, three and one additional zinc finger motifs, in contrast to the bovine counterpart expressed in retina and liver. Zinc finger domains 5 and 6 of HeLa RanBP2 are 100% identical to each other. Zinc finger 4 of HeLa RanBP2 represents likely the additional domain not present in the bovine RanBP2 because, in contrast to HeLa, a stretch of 15 nucleotides was absent. RanBP2 of the murine F9 cell line has six zinc finger motifs. A large part of the downstream sequence flanking the murine 3rd Zn^{2+} finger is missing and the 4th Zn^{2+} finger appears to be an exogenous inserted sequence since it is missing in the bovine counterpart. The cysteine codon (TG(T/C)) parts of the Zn^{2+} motifs, tryptophan (TGG, first codon) and asparagine (AAT, in the middle of the zinc finger loop) codons, are 100% conserved in all Zn^{2+} fingers, with the exception of the bovine 4th zinc finger which is missing the second cysteine. The conserved tryptophan (*boxed*), asparagine (*shaded dark gray*), and cysteine (*shaded light gray*) codons (*A*) and amino acids (*B*) are shown. The bovine Zn-sequence was deposited in GenBank™ with accession number AJ133723. *Numerals* before the Zn-motifs of each species refer to the identity of each zinc finger; *Bov*, bovine.

this end, RBD4 had no effect on the interaction of ZnF-BP with GST-ZnF (Fig. 3*b*). Then we determined the effect of nonhydrolyzable nucleotides in the binding of retinal ZnF-BP to RanBP2 because we had previously shown a nucleotide-dependent interaction of Ran-GTPase, 19 S regulatory subunits of the proteasome and a putative kinesin with RanBP2 (2). Association of ZnF-BP to GST-ZnF, however, was independent of the presence of the nucleotide analogues, GTPγS, ATPγS, and AMP-PNP (Fig. 3*a*).

The biological activity of zinc finger-containing proteins critically depends on the presence of Zn^{2+} for the formation of properly folded and active proteins (53). Thus, we investigated whether binding of retinal ZnF-BP to GST-ZnF required the presence of Zn^{2+}. To this end, we compared the degree of release of ZnF-BP from GST-ZnF in the presence of a ubiquitous chelator, EDTA, and selective heavy metal chelator, *N,N,N′,N′*-tetrakis(2-pyridylmethyl)ethylenediamine (TPEN) (54–57). SDS-PAGE analysis of the supernatants, obtained upon addition of EDTA or TPEN to washed GST-ZnF retinal coprecipitates, showed the specific release to the supernatant of just the 110-kDa ZnF-BP (Fig. 3*c*). In comparison with EDTA, this dissociation was increased and almost complete in the presence of 10-fold lower concentration of TPEN (Fig. 3*c*, *2nd* and *3rd lanes*). Then we investigated whether Zn^{2+} would specifically lead to the reassociation of ZnF-BP with GST-ZnF after its release by TPEN. Indeed, addition of excess molar

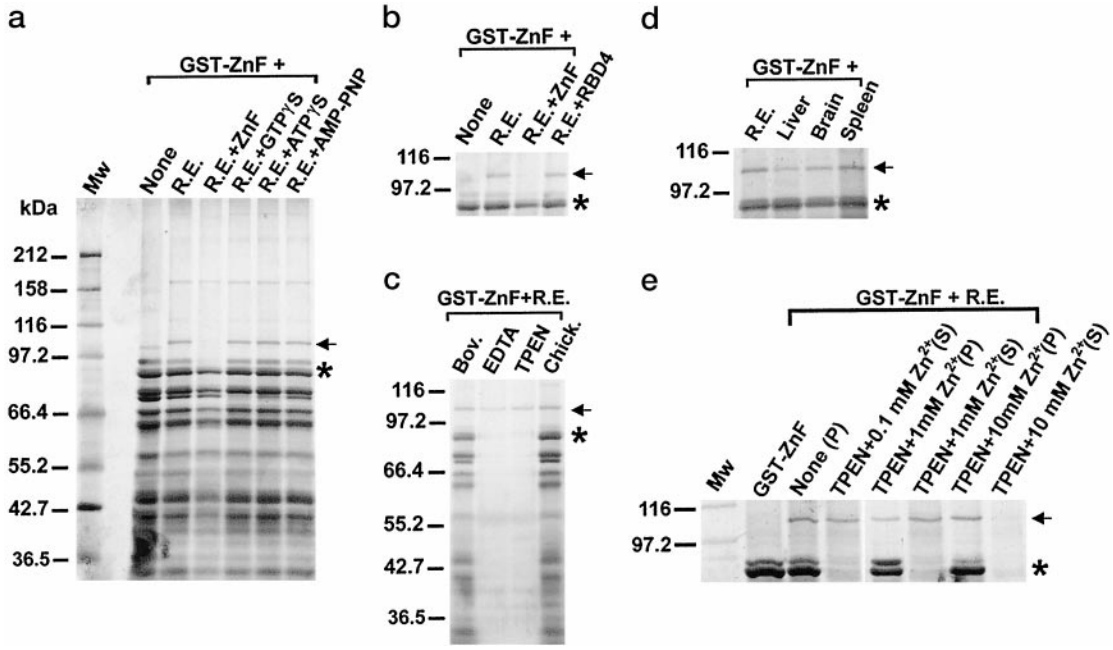

FIG. 3 *a,* silver stain SDS-PAGE analysis of glutathione *S*-agarose coprecipitates of bovine (*Bov.*) retinal incubation reactions with GST-ZnF of bovine retinal RanBP2 led to the identification of a 110-kDa retinal protein that associates specifically with ZnF domain of RanBP2. Incubation of GST-ZnF with retinal extracts led to the association of several proteins to the fusion protein (*3rd lane*). Among these, only a retinal protein with an apparent molecular mass of 110 kDa associated specifically with the ZnF moiety of the fusion protein because this was the only protein whose binding to GST-ZnF was completely disrupted in the presence of free (unfused) ZnF (*4th lane*). There was also a protein of approximately 95 kDa that was partially competed off in the presence of competitor. However, this protein was also present in purified GST-ZnF alone (*2nd lane*) and thus, the competition of this protein by ZnF represents an artifact because it was not often reproducible in other experiments (see Figs. 3*d* and 4). Association of this 110-kDa retinal protein to ZnF was independent of the presence of GTPγS (*5th lane*), ATPγS (*6th lane*), and AMP-PNP (*7th lane*). Western blot analysis of purified GST-ZnF with two affinity purified polyclonal antibodies against ZnF and another against GST confirmed that the protein species below GST-ZnF (seen in *2nd lane*) are degradation products of the purified GST fusion protein.[3] *1st lane*, molecular weight standards. *b,* the retinal 110-kDa ZnF protein associates specifically with ZnF domain of RanBP2. Silver stain SDS-PAGE analysis of retinal GST-ZnF coprecipitates showed that binding of ZnF-BP to GST-ZnF (*2nd lane*) was completely blocked in the presence of unfused ZnF (*3rd lane*) but not by the unrelated domain of RanBP2, RBD4 (*4th lane*). *c,* association of ZnF-BP to ZnF domain of retinal RanBP2 is dependent on Zn^{2+} stabilization of Zn^{2+} finger secondary structures and is species-independent. The retinal ZnF-BP could be partially dissociated from GST-ZnF coprecipitates and released to the supernatant in the presence of 50 mM of the broad EDTA chelator (*2nd lane*). This dissociation was almost complete in the presence of 5 mM of the Zn^{2+} chelator, TPEN. Strong association of ZnF-BP to GST-ZnF was also observed in the extracts prepared from cone-rich chicken retinas (*4th lane*). The total amount of extract protein used was half that of bovine extracts. *d,* the ZnF-BP is expressed ubiquitously. The 110-kDa ZnF-BP coprecipitated with GST-ZnF in liver (*2nd lane*), brain (*3rd lane*), and spleen (*4th lane*) with similar affinity to that observed in retinal extracts (*1st lane*). All protein tissue extract concentrations were normalized to that used in retinal extract reactions. *e,* GST-ZnF and ZnF-BP binary complex is reconstituted in the presence of excess molar of Zn^{2+}. GST-ZnF retinal coprecipitates were incubated in the absence or presence of 1 mM TPEN followed by incubation with increasing concentrations of Zn^{2+}. Pellets (*P*) and supernatants (*S*) of incubation reactions were then analyzed on SDS-PAGE and silver stain. In the presence of 10 mM Zn^{2+} all ZnF-BP reassociates with ZnF domain of RanBP2 (*7th* and *8th lanes*). *asterisk*, intact GST-ZnF; *arrow*, retinal ZnF-binding protein (ZnF-BP); *R.E.,* bovine retinal extracts.

Zn^{2+} (10 mM) to the elution reactions led to the complete reassociation of ZnF-BP with GST-ZnF (Fig. 3*e*, *7th* and *8th lanes*), in contrast to that of the addition of just 0.1 and 1 mM Zn^{2+} (Fig. 3*e*, *4th to 6th lanes*).

Finally, we had previously shown that association of RanBP2 to the 19 S regulatory subunits of the proteasome was selective for the retina. To this end, we determined whether association of Zn-BP to zinc domain of RanBP2 was tissue-specific and also species-specific by incubating GST-ZnF with extracts from other tissue sources and chicken retinas. These were normalized to the concentrations of those used in bovine retinal extracts. As shown in Fig. 3, *d*, and *c* (*4th lane*) respectively, GST-ZnF associated with ZnF-BP from bovine liver, brain, and spleen as well as cone-rich chicken retinas.

Purification of RanBP2 Zinc Finger-binding Protein—To determine the identity of ZnF-BP, we scaled up the analytical incubation reactions 500-fold and purified ZnF-BP. GST-ZnF retinal coprecipitates were extensively washed, and retinal ZnF-BP was specifically eluted from GST-ZnF·ZnF-BP complex by addition of EDTA/TPEN (50:1) and DTT followed by SDS-PAGE and electroelution of purified ZnF-BP by methods similar to those previously reported (2, 4). We confirmed the large scale purification of ZnF-BP by running a small aliquot of purified ZnF-BP (5% v/v) in parallel with analytical reactions (Fig. 4). The remaining purified protein and a mock SDS-PAGE sample were then subjected to trypsin digestion. Then we carried out MALDI-TOF mass mapping on an aliquot of the tryptic peptide mixture followed by data base searches. CRM1/Exportin1 (45, 47–50, 58) was tentatively identified as the 110-kDa ZnF-BP because the masses of all peptides isolated and identified matched those predicted from the tryptic digest of exportin-1 (not shown). To confirm further exportin-1 as the retinal ZnF-BP, the remaining tryptic peptide mixture of the 110-kDa ZnF-BP was resolved on HPLC, and all fractions collected were screened by mass spectrometry. Only those appearing to contain clean molecular species were subjected to Edman degradation. Amino acid sequence analysis of fractions 53 and 37 yielded three peptide sequences of 16, 19, and 14 amino acids (Fig. 5). An arginine preceded all three peptides reported in the counterpart human sequence, and all bovine peptides ended with an arginine or lysine as expected from a trypsin digestion. Comparison of these sequences against other proteins in the data base matched 100% counterpart sequences of human chromosome maintenance region 1 protein (hCRM1) (48, 58) (Fig. 5), confirming the results obtained initially by MALDI peptide mapping. This protein was recently renamed, exportin-1 (and

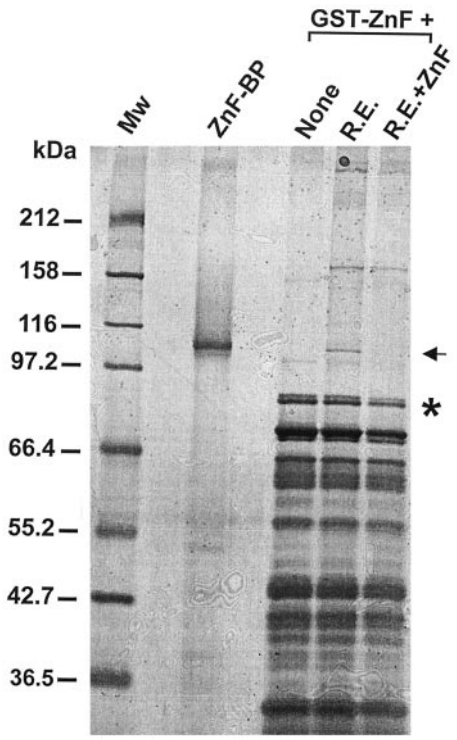

FIG. 4. **Purification of 110-kDa retinal ZnF-binding protein.** Retinal incubation reactions were scaled up, and the ZnF-BP was eluted from the GST-ZnF·ZnF-BP complex with EDTA/TPEN (50:1). Eluted protein was resolved on SDS-PAGE, electroeluted, and concentrated, and an aliquot was loaded on SDS-PAGE (*2nd lane*), in parallel with analytical incubation reactions for silver stain analysis (*3rd* to *5th lanes*). The purified retinal protein migrated exactly to that observed in analytic incubation reactions. *R.E.,* bovine retinal extracts; *arrow,* retinal ZnF-binding protein (*ZnF-BP*).

Bovine Peptide #53: 1 AIIASNIMYIVGQYPR 17
Human CRM1: 537 (R)AIIASNIMYIVGQYPR 553

Bovine Peptide #37A: 1 MAKPEEVLVVENDQGEVVR 20
Human CRM1: 423 (R)MAKPEEVLVVENDQGEVVR 442

Bovine Peptide #37B: 1 VXTILEFSQNMNTK 15
Human CRM1: 62 (R)VDTILEFSQNMNTK 76

FIG. 5. **Tryptic peptides of ZnF-BP and sequence comparison with human exportin-1/CRM1.** Three peptides were isolated by HPLC from trypsin digestion of purified ZnF-BP and identified by MALDI scanning. Edman degradation and sequence comparison analysis of these peptides with other proteins in the data base revealed that they were identical to the human CRM1 (exportin-1) protein. HPLC fraction 37 contained two peptides identical to CRM1. Arginines in *parentheses* represent human residues preceding the first residue sequenced in bovine peptides by Edman degradation and are sites of trypsin cleavage. *X*, amino acid residue not determined likely due to a post-translational modification.

is hereafter referred as such), in light of its role in the export of substrates from the nucleus to the cytoplasm (50).

Association of CRM1/Exportin-1 to the Zinc Finger Motifs of RanBP2 Is Leptomycin B-insensitive—Leptomycin B (LMB) (59, 60) is an antibiotic leading to cell cycle arrest in yeast and mammalian cells (61, 62). It also inhibits the nuclear export of human immunodeficiency virus, type I, Rev protein and human immunodeficiency virus, type I-dependent pre-mRNA (63). Recently, LMB was found to be a potent and specific inhibitor of NES-dependent export of nuclear proteins by binding directly to exportin-1 and abolishing its association with NES-containing substrates (46–49). Formation of NES·exportin-1 complex has also been shown to require Ran in a GTP-bound state (46). LMB was shown to disrupt the formation of this ternary complex including Ran-GTP cooperative interaction with exportin-1 (46). For these reasons, we investigated the behavior of Ran-GTPase in the formation of exportin-1·ZnF complex in the presence and absence of LMB and/or guanine nucleotides and the effect of LMB in the docking reaction of exportin-1 to the ZnF domain of RanBP2.

To this end, we carried out retinal incubation reactions in the presence of GST-ZnF and observed the effect of LMB activity, guanine nucleotide analogues, singly or in combination, in the interaction of exportin-1 and Ran-GTPase with bovine GST-ZnF of RanBP2. These reactions were carried out in the presence of the proteasome inhibitors, lactacystine and MG-132, to prevent potential activation of the proteasome machinery by components of the Ran-GTPase cycle (2, 64). Fig. 6, *a* and *b,* show Western blot analysis of the same retinal GST-ZnF coprecipitates with antibodies against exportin-1 (Fig. 6*a*) and Ran-GTPase (Fig. 6*b*). As seen in Fig. 6*a*, association of exportin-1 with ZnF of RanBP2 did not change significantly in the presence of leptomycin B (*4th lane*) and the nucleotide analogues, GTPγS (*3rd lane*) and GDPβS (*7th lane*), compared with those in the absence of these (*2nd* and 6th *lane*s). In contrast, when the same retinal coprecipitates were analyzed for the effect of these factors in Ran-GTPase association with ZnF·exportin-1 complex, we observed that Ran interaction with this complex was significantly decreased by GTPγS (*3rd lane*) and LMB (*4th lane*). The combination of these two reagents appeared to have a slight synergistic effect on Ran association with ZnF·exportin-1 (*5th lane*). Addition of GDPβS to the retinal incubation reactions led just to a slight decrease in Ran binding to the complex (*7th lane*). The leptomycin B solvent, dimethyl sulfoxide, by itself, had no effect on Ran association with the binary complex (*6th lane*).

We have previously shown that the RBD4-CY supradomain of RanBP2 associates with Ran with high affinity in a GTP-dependent and CY-independent manner (3–4). We compared the relative amount of Ran that associated with the binary complex, ZnF domain of RanBP2 and exportin-1, to that with RBD4-CY. This also helped to confirm the GTP loading and guanine nucleotide-dependent binding of Ran to these substrates. To this purpose, control reactions with retinal extracts were carried out with 10-fold lower concentrations of RBD4-CY in the presence or absence of guanine nucleotide analogues (Fig. 6*d*). As shown in Fig. 6*c*, RBD4-CY does not interact with exportin-1. However, Ran interaction with RBD4 occurs in a GTP-dependent fashion and with very high affinity even when GST-RBD4-CY was used at 10-fold lower concentration compared with that of GST-fused ZnF (*e.g.* compare *2nd* and *4th lanes* of Fig. 6*d* with *2nd* and *7th lanes* of Fig. 6*b*).

DISCUSSION

In this report, evidence is now provided that the zinc finger cluster domain of RanBP2 associates specifically to a key nuclear export factor, exportin-1 (45–50). Like other Zn^{2+} finger homologous domains (53), this binding is dependent on the structural integrity of the Zn^{2+} finger domain and presence of Zn^{2+}. Removal of Zn^{2+} from this domain reversibly destroys its ability to associate with exportin-1. In contrast to CLD of RanBP2 (2), association of exportin-1 with ZnF domain is independent of the presence of nucleotides (Figs. 3*a* and 6, *a* and *e*) and is observed across different tissues (Fig. 3*d*) and species (Fig. 3*c*). Furthermore, the formation of the binary complex, ZnF·exportin-1, is insensitive to leptomycin B, a cytotoxin shown to uncouple the cooperative binding of nuclear cargo and Ran-GTP from exportin-1 (46). It has been proposed that this is

[3] B. B. Singh, H. H. Patel, and P. A. Ferreira, unpublished observations.

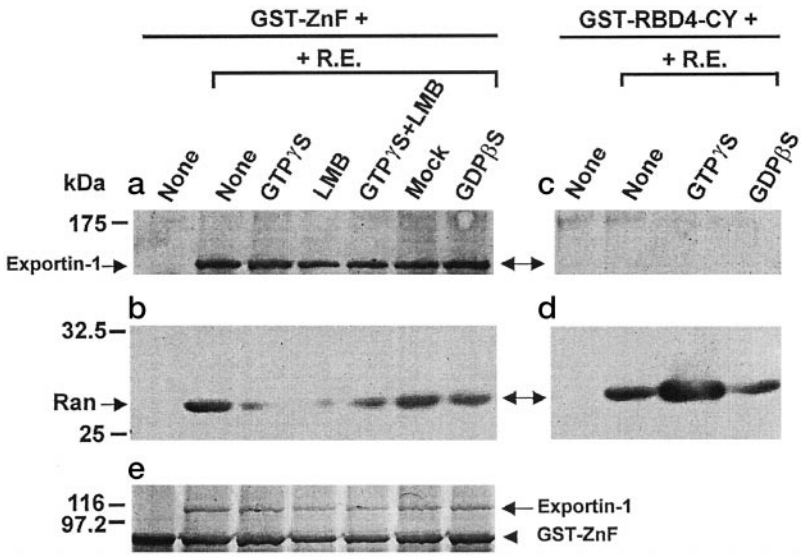

FIG. 6. **Association of ZnF of RanBP2 with exportin-1/CRM1 is leptomycin B- and guanine nucleotide-insensitive.** Ran-GTPase forms a ternary complex with ZnF of RanBP2 in a GDP-dependent manner. Retinal incubation reactions with bovine GST-ZnF were carried out as described. GST-ZnF coprecipitates were eluted with SDS sample buffer, and half was analyzed by SDS-PAGE silver staining and the other half by Western blot analysis. *a,* Western blot analysis of bovine GST-ZnF coprecipitates from retinal extracts with an antibody against exportin-1/CRM1. GST-ZnF pulled down analytical assays were carried out in the presence or absence of leptomycin B (*LMB*) and nonhydrolyzable guanine nucleotide analogues. Leptomycin B and nonhydrolyzable guanine nucleotide analogues had largely no effect on the specific association of exportin-1/CRM1 with ZnF domain of RanBP2 (*3rd* to *5th* and *7th lanes*). In the mock binding assay, only LMB solvent (Me_2SO) was used (*6th lane*). *b,* Western blot analysis of the same bovine GST-ZnF coprecipitates from retinal extracts (shown in *a*) with an antibody against Ran-GTPase. Ran associates with the binary complex, ZnF of RanBP2 and exportin-1, in a leptomycin B- (*4th lane*) and GTP (*3rd lane*)-sensitive fashion. *c* and *d* are, respectively, Western blot analysis of GST-RBD4/CY coprecipitates from retinal extracts with antiserum against exportin-1 and Ran. Exportin-1 does not associate with GST-RBD4-CY under any of the conditions shown (*c*). In contrast to GST-ZnF, Ran interacts with RBD4-CY in a GTP-dependent fashion (compare *3rd* and *4th lanes* of *d*) and significantly higher affinity. *e,* SDS-PAGE silver stain analysis of control reactions of bovine GST-ZnF (*GST-ZnF*) coprecipitates from retinal extracts. *R.E.*, bovine retinal extracts.

achieved by blocking the cooperative association of Ran-GTP (46) and NES present in cargo proteins to exportin-1 (46–49). The data presented here indicate that the leptomycin B-binding site in exportin does not overlap with its ZnF binding domain. Thus, these results suggest that exportin-1 contains distinct NES and ZnF receptor domains. The interaction of the N terminus of importin-β with Ran (34) and homology of the N terminus of exportin-1 with this domain, commonly designated as the CRIME domain (58), also support that the Zn-F docking domain in exportin-1 likely lies outside its N terminus. Finally, while this manuscript was under revision, two reports by Kudo *et al.* (65) and Neville and Rosbash (66) have shown that a single cysteine, located in the central conserved region (CCR) of exportin-1 and conserved among LMB-sensitive organisms, was the residue responsible for determining LMB sensitivity to exportin-1. Thus, its also unlikely that this region contributes to the docking reaction of exportin-1 to RanBP2. Based on these results, the RanBP2 docking domain in exportin-1 may lay between the CRIME and CCR domains and/or on the C-terminal domain downstream of CCR.

We have also found that Ran was part of the exportin-1·ZnF complex. In contrast to exportin-1, this association, however, was significantly decreased by the presence of the non-hydrolyzable analogue, GTPγS (Fig. 6*b, 3rd lane 3*), or leptomycin B (Fig. 6*b, 4th lane*). The GDP-dependent Ran association with the exportin·ZnF complex appears to be consistent with current models whereby Ran-GTP export from the nucleus leads ultimately to hydrolysis of GTP. Thus, Ran-GTP hydrolysis may be required to disassemble the nuclear cargo from exportin-1 before or upon docking of exportin-1 to the ZnF domain of RanBP2. This would lead to Ran dissociation from exportin-1 and its possible transfer to the ZnF domain of RanBP2 and/or a closely linked component part of the RanBP2 macroassembly complex. In support of this hypothesis is also the observation that the counterpart ZnF domain of human RANBP2 (with and without the C-terminal junction sequence between ZnF and RBD2) still associates with Ran but not with exportin-1.[3] This latter effect is most likely due to partial misfolding of this significantly larger recombinant isoform.

Leptomycin B also led to a drastic reduction, in the absence of GTP, of binding of Ran to the binary complex comprised by ZnF domain of RanBP2 and exportin-1 (Fig. 6, *4th lane*). This result is apparently unexpected if we consider, as described, the GTP-dependent and leptomycin B-sensitive association of Ran with exportin-1. One possible explanation is that binding of exportin-1 to leptomycin B also inhibits by steric hindrance the association of Ran-GDP (or free nucleotide Ran) to a Ran-GDP binding domain within the ZnF domain of RanBP2. This may be due to a reported conformational change of exportin-1 upon leptomycin B binding (46). Thus, leptomycin B may have a dual effect; it inhibits the cooperative formation of a competent nuclear cargo complex and the apparent weaker association (in comparison with exportin-1) of Ran-GDP with RanBP2 docking complex. These results appear to be in partial agreement with the data of a recent report published while this manuscript was under review where the recombinant zinc finger domain of human RANBP2 was shown to associate exclusively with recombinant Ran-GDP but not Ran-GTP (67). However, further studies need to be carried out to determine whether this association is, indeed, specific.

It remains unclear whether there is any functional significance for the presence of one and three additional zinc fingers in the mouse and human RANBP2 isoforms, respectively (Fig. 2). To narrow down the exportin-1-binding domain in RanBP2, we have attempted the expression of several Zinc finger bovine and human mutant constructs. However, these proved difficult to express or obtain in a folded competent form. Furthermore, it is interesting to note that the human 5th and 6th zinc finger motifs and flanking nucleotide sequences are 100% identical to each other suggesting a very recent genetic duplication in hu-

mans. In any case, the extra zinc fingers of human and mouse may likely play a redundant role in the association of the ZnF domain of RanBP2 with exportin-1 and Ran-GDP.

Nucleoporins are also characterized for the presence of small peptide motifs (11). The repeat, F*X*FG, is present throughout the RanBP2 sequence as well as some other nucleoporins such as CAN/NUP214 (68) and NUP153 (69, 70). These are localized at the cytoplasmic and nucleoplasmic face of the nuclear pore complex, respectively. NUP153 is the only other nucleoporin known to contain a zinc finger cluster domain homologous to the RanBP2 counterpart domain (5) and proposed to associate with nuclear DNA based on its ability to bind DNA *in vitro* (69). The F*X*FG repeats have also been postulated to constitute sites for stochastic docking and undocking reactions potentially required for the nucleocytoplasmic translocation (in a saltatory fashion) of importin-β-like transport factors (43). In this respect, the yeast F*X*FG sequences of Nup and Nup2 nucleoporins have been shown to associate *in vitro* with karyopherin heterodimers (43). In analogy to this model, it is thought that nuclear export of exportin-1 may undergo a similar mechanism. This is supported by the fact that exportin-1 associates with the C-terminal domain of CAN/NUP214 that contains F*X*FG repeats (58).

Nevertheless, it is difficult to conceive the vectorial transport of substrates primarily through a stochastic mechanism even in the presence of an asymmetric distribution of Ran-bound nucleotide for the following reasons. We have shown that different RanBP2 domains, also containing F*X*FG motifs, associate in a rather stable and, more importantly, specific fashion, with red opsin (3, 6), Ran (3, 4), 19 S regulatory particle of the proteasome (2), and some other tissue-restricted proteins.[4] Formation of these complexes will likely prevent the "axial" movement of nuclear escort factors and associated cargo through these repeat "tracks" due to steric hindrance. The formations of zinc finger motifs and unique primary sequences are crucial for the specific binding of exportin-1 to the ZnF domain of RanBP2 (Figs. 2*c* and 6α). Although one cannot yet exclude that the FG motifs may contribute to the lowering of the overall free-binding energy (*e.g.* avidity) of substrates to these domains, our data support that they are not the primary determinants for the formation of such complexes. This is further supported by data obtained from the yeast FG-containing nucleoporin, Rip1p, that has been shown to mediate nuclear export independently of its FG repeat motifs (71) and unsuccessful attempts to show the influence of FG repeats in the formation of exportin-1·NES complex (46). Finally, in view of the strong homology between zinc finger clusters of RanBP2 and NUP153 (5), our data suggest that NUP153 (69) may possess a specific docking site for exportin-1 (*e.g.* during recycling) or other importin-β-like receptor factors at the nucleoplasmic face of the NPC. This appears, indeed, to be the case. During the course of the review of this work, Nakielny *et al.* (72) reported that the homologous ZnF domain of NUP153 associates with Ran in a GDP-dependent fashion. Moreover, NUP153 appears to mediate antagonistic export and import receptor interactions with Ran-GTP (72).

Our results indicate that RanBP2 is a primary component of the nuclear export pathway. This is in contrast to another report where RanBP2 was shown to mediate nuclear import (5). Despite RanBP2 and NUP214/CAN association with exportin-1, they are likely part of separate nuclear transport pathways as RanBP2 does not appear to copurify with NUP214/CAN, and exportin-1 still localizes at the nuclear envelope in *can*$^{-/-}$ knockout mouse embryos (58). Finally, our results outline a picture where RanBP2 emerges as a primary candidate in mediating the translocation of nuclear cargo to cytoplasmic machinery such as the 19 S regulatory particle of the proteasome. An analogous pathway has been proposed to occur during nuclear export of the specific premessenger ribonucleoprotein complexes, the Balbiani ring particles, in the salivary glands of *Chironomus tentans* (73, 74). In light of RanBP2-dependent production of red/green opsins (3, 6) and high expression in cone photoreceptors (75), it is interesting to note that the highly expressed cognate transcripts of red/green opsins have also been localized at the perinuclear region of cone photoreceptors (76). This is in contrast to the broad cytoplasmic distribution of their counterpart rhodopsin transcript in rod photoreceptors (76). Further identification and characterization of the components associated with RanBP2 macroassembly complex will provide us with a framework to understand the molecular mechanisms associated with nucleocytoplasmic transport of mRNAs and their translation in photoreceptors.

Acknowledgments—We thank Jerry Shay (University of Texas, SW) for HeLa cells, Minoru Yoshida (University of Tokyo) and Barbara Wolff (Novartis, Austria) for leptomycin B, Gerard Grosveld (St. Judes Children Research Hospital) for CRM1/exportin-1 antiserum, and Michael Pereckas and Xuegong Zhu for protein and MALDI-MS analysis.

REFERENCES

1. Alberts, B. (1998) *Cell* **92,** 291–294
2. Ferreira, P., Yunfei, C., Schick, D., and Roepman, R. (1998) *J. Biol. Chem.* **273,** 24676–24682
3. Ferreira, P., Nakayama, T., Pak, W., and Travis, G. (1996) *Nature* **383,** 637–640
4. Ferreira, P. (2000) *Methods Enzymol.,* **315,** 455–468
5. Yokoyama, N., Hayashi, N., Seki, T., Pante, N., Ohba, T., Nishil, K., Kuma, K., Hayashida, T., Miyata, T., Aebi, U., Fuki, M., and Nishimoto, T. (1995) *Nature* **376,** 184–188
6. Ferreira, P., Nakayama, T., and Travis, G. (1997) *Proc. Natl. Acad. Sci. U. S. A.* **94,** 1556–1561
7. Saitoh, H., Pu, R., Cavenagh, M., and Dasso, M. (1997) *Proc. Natl. Acad. Sci. U. S. A.* **94,** 3736–3741
8. Mahajan, R., Delphin, C., Guan, T., Gerace, L., and Melchior, F. (1997) *Cell* **88,** 97–107
9. Mahajan, R., Gerace, L., and Melchior, F. (1997) *J. Cell Biol.* **140,** 259–270
10. Manutis, M., Coutavas, E., and Blobel, G. (1997) *J. Cell Biol.* **135,** 1457–1470
11. Davis, L. I. (1995) *Annu. Rev. Biochem.* **64,** 865–896
12. Wu, J., Matunis, J., Kraemer, D., Blobel, G., and Coutavas, E. (1995) *J. Biol. Chem.* **270,** 14209–14213
13. Siniossoglou, S., Wimmer, C., Rieger, M., Doye, V., Tekotte, H., Weise, C., Emig, S., Segref, A., and Hurt, E. C. (1996) *Cell* **84,** 265–275
14. Pryer, N. K., Salama, N. R., Schekman, R. W., and Kaiser, C. A. (1993) *J. Cell Biol.* **120,** 865–875
15. Wilken, N., Senecal, J.-L., Scheer, U., Dabauvalle, M.-C. (1995) *Eur. J. Cell Biol.* **68,** 211–219
16. Melchior, F., Guan, T., Yokoyama, N., Nishimoto, T. and Gerace, L. (1995) *J. Cell Biol.* **131,** 571–581
17. Coutavas, E., Ren, M., Oppenheim, D., D'Eustachio, P., and Rush, M. G. (1993) *Nature* **366,** 585–587
18. Lounsbury, K. M., Beddow, A. L., and Macara, I. G. (1994) *J. Biol. Chem.* **269,** 11285–11290
19. Bischoff, F. R., Krebber, H., Smirnova, E., Dong, W., and Ponstingl, H. (1995) *EMBO J.* **14,** 705–715
20. Beddow, A. L., Richards, S. A., Orem, N. R., and Macara, I. G. (1995) *Proc. Natl. Acad. Sci. U. S. A.* **92,** 3328–3332
21. Dasso, M., and Pu, R. T. (1998) *Am. J. Hum. Genet.* **63,** 311–316
22. Moore, M. S. (1998) *J. Biol. Chem.* **273,** 22857–22860
23. Ohno, M., Fornerod, M., and Mattaj, I. W. (1998) *Cell* **92,** 327–336
24. Moore, M. S., and Blobel, G. (1993). *Nature* **365,** 661–663
25. Melchior, F., Paschal, B., Evans, J., and Gerace, L. (1993) *J. Cell Biol.* **123,** 1649–1659
26. Moroianu, L., and Blobel, G. (1995) *Proc. Natl. Acad. Sci. U. S. A.* **92,** 4318–4322
27. Izaurralde, E., Kutay, U., von Kobbe, C., Mattaj, I. W., and Gorlich, D. (1997) *EMBO J.* **16,** 6535–6547
28. Richards, S. A., Carey, K. L., and Macara, I. G. (1997) *Science* **276,** 1842–1844
29. Jans, D. A., and Hubner, S. (1996) *Physiol. Rev.* **76,** 651–685
30. Fischer, U., Huber, J., Boelens, W. C., Mattaj, I. W., and Luhrmann, R. (1995) *Cell* **82,** 475–483
31. Wen, W., Meinkoth, J. L., Tsien, R. Y., and Taylor, S. S. (1995) *Cell* **82,** 463–473
32. Murphy, R., and Wente, S. R. (1996) *Nature* **383,** 357–360
33. Arenzana-Seisdedos, F., Turpin, P., Rodriguez, M., Thomas, D., Hay, R. T., Virelizier, J. L., Dargemont, C. (1997) *J. Cell Sci.* **110,** 369–378
34. Gorlich, D. (1997) *Curr. Opin. Cell Biol.* **9,** 412–419
35. Ullman, K. S., Powers, M. A., and Forbes, D. J. (1997) *Cell* **90,** 967–970
36. Brinkmann, U., Brinkmann, E., Gallo, M., and Pastan, I. (1995) *Proc. Natl. Acad. Sci. U. S. A.* **92,** 10427–10431

[4] B. B. Singh and P. A. Ferreira, manuscript in preparation.

37. Kutay, U., Bischoff, F. R., Kostka, S., Kraft, R., and Gorlich, D. (1997) *Cell* **90,** 1061–1071
38. Aitchison, J. D., Blobel, G., and Rout, M. P. (1996) *Science* **274,** 624–627
39. Pollard, V. W., Michael, W. M., Nakielny, S., Siomi, M. C., Wang, F., and Dreyfuss, G. (1996) *Cell* **86,** 985–994
40. Siomi, H., and Dreyfuss, G. (1995) *J. Cell Biol.* **129,** 551–560
41. Michael, W. M., Choi, M., and Dreyfuss, G. (1995) *Cell* **83,** 415–422
42. Gorlich, D., Pante, N., Kutay, U., Aebi, U., and Bishoff, F. R. (1996) *EMBO J.* **15,** 5584–5594
43. Rexach, M., and Blobel, G. (1995) *Cell* **83,** 683–692
44. Radu, A., Moore, M. S., and Blobel, G. (1995) *Cell* **81,** 215–222
45. Adachi, Y., and Yanagida, M. (1989) *J. Cell Biol.* **108,** 1195–1207
46. Fornerod, M., Ohno, M., Yoshida, M., and Mattaj, I. W. (1997) *Cell* **90,** 1051–1060
47. Fukuda, M., Asano, S., Nakamura, T., Adachi, M., Yoshida, M., Yanagida, M., and Nishida, E. (1997) *Nature* **390,** 308–311
48. Kudo, N., Khochbin, S., Nishi, K., Kitano, K., Yanagida, M., Yoshida, M., and Horinouchi, S. (1997) *J. Biol. Chem.* **272,** 29742–29751
49. Ossareh-Nazari, B., Bachelerie, F., and Dargemont, C. (1997) *Science* **278,** 141–144
50. Stade, K., Ford, C. S., Guthrie, C., and Weis, K. (1997) *Cell* **90,** 1041–1050
51. Krebber H. Bastians H. Hoheisel J. Lichter P. Ponstingl H. Joos S. (1997) *Genomics* **43,** 247–248
52. Nothwang, H. G., Rensing, C., Kubler, M., Denich, D., Brandl, B., Stubanus, M., Haaf, T., Kurnit, D., and Hildebrandt, F. (1998) *Genomics* **47,** 383–392
53. Klug, A., and Schwabe, J. W. (1995) *FASEB J.* **9,** 597–604
54. Anderegg, G., and Wenk, F. (1967) *Helv. Chim. Acta* **50,** 2330–2332
55. Herketh, T. R., Smith, G. A., Moore, J. P., Taylor, M. V., and Metcalfe, J. C. (1983*) J. Biol. Chem.* **258,** 4876–4882
56. Cheng, C., and Reynolds, I. J. (1998) *J. Neurochem.* **71,** 2401–2410
57. Fekkes, P., Wit, J., Boorsma, A., Friesen, R., and Driessen, A. (1999) *Biochemistry* **38,** 5111 -5116
58. Fornerod, M., Deursen, J. V., van Baal, S., Reynolds, A., Davis, D., Murti, K. G., Fransen, J., and Grosveld, G. (1997) *EMBO J.* **16,** 807–816
59. Hamamoto, T., Gunji, S., Tsuji, H., and Beppu, T. (1983) *J. Antibiotics* **XXXVI,** 639–645
60. Hamamoto, T., Seto, H., and Beppu, T. (1983) *J. Antibiotics* **XXXVI,** 646–650
61. Hamamoto, T., Uozumi, T., and Beppu, T. (1985) *J. Antibiotics* **XXXVIII,** 1573–1580
62. Yoshida, M., Nishikawa, M., Nishi, K., Abe, K., Horinouchi, S., and Beppu, T. (1990) *Exp. Cell Res.* **187,** 150–156
63. Wolff, B., Sangler, J. J., and Wang, Y. (1997) *Chem. Biol.* **4,** 139–147
64. Desterro, J., Rodriguez, M., and Hay, R. (1998) *Mol. Cell* **2,** 233–239
65. Kudo, N., Matsumori, N., Taoka, H., Fujiwara, D., Shreiner, E., Wolff, B., Yoshida, M., and Horinouchi, S. (1999) *Proc. Natl. Acad. Sci. U. S. A.* **96,** 9112–9117
66. Neville, M., and Rosbash (1999) *EMBO J.* **18,** 3749–3756
67. Yaseen, N., and Blobel, G. (1999) *Proc. Natl. Acad. Sci. U. S. A.* **96,** 5516–5521
68. Fornerod, M., Boer, J., van Baal, S., Morreau, H., and Grosveld, G. (1996) *Oncogene* **13,** 1801–1808
69. Sukegwa, J., and Blobel, G. (1993) *Cell* **72,** 29–38
70. McMorrow, I., Bastos, R., Horton, H., and Burke, B. (1994) *Biochim. Biophys. Acta* **1217,** 219–223
71. Stutz, F., Kantor, J., Zhang, D., McCarthy, T., Neville, M., and Rosbash, M. (1997) *Genes Dev.* **11,** 2857–2868
72. Nakielny, S., Shaikh, S., Burke, B., and Dreyfuss, G. (1999) *EMBO J.* **18,** 1982–1995
73. Visa, N., Alzhanova-Ericsson, A. T., Sun, X., Kiseleva, E., Bjorkroth, B., Wurtz, T., and Daneholt, B. (1996) *Cell* **84,** 253–264
74. Daneholt, B. (1997) *Cell* **88,** 585–588
75. Ferreira, P., Hom, J., and Pak, W. (1995) *J. Biol. Chem.* **270,** 23179–23188
76. Raymond, P. A., Barthel, L. K., Rounsifer, M. E., Sullivan, S. A., and Knight, J. K. (1993) *Neuron* **10,** 1161–1174
77. Guan, K. L., and Dixon, J. E. (1991) *Anal. Biochem.* **192,** 262–267